

The Shapes of Galaxies in the Sloan Digital Sky Survey

S. M. Khairul Alam & Barbara S. Ryden

Department of Astronomy, The Ohio State University

140 W. 18th Avenue, Columbus, OH 43210

alam, ryden@astronomy.ohio-state.edu

ABSTRACT

We estimate the distribution of apparent axis ratios q for galaxies in the Sloan Digital Sky Survey (SDSS) Early Data Release. We divide the galaxies by profile type (de Vaucouleurs versus exponential) as well as by color ($u^* - r^* \leq 2.22$ versus $u^* - r^* > 2.22$). The axis ratios found by fitting models to the surface photometry are generally smaller than those found by taking the second moments of the surface brightness distribution. Using the axis ratios found from fitting models, we find that galaxies with de Vaucouleurs profiles have axis ratio distributions which are inconsistent, at the 99% confidence level, with their being a population of randomly oriented oblate spheroids. Red de Vaucouleurs galaxies are slightly rounder, on average, than blue de Vaucouleurs galaxies. By contrast, blue galaxies with exponential profiles appear very much flatter, on average, than red galaxies with exponential profiles. The red exponential galaxies are primarily disk galaxies seen nearly edge-on, with reddening due to the presence of dust, rather than to an intrinsically red stellar population.

Subject headings: galaxies: elliptical and lenticular, cD – galaxies: spiral – galaxies: photometry – galaxies: fundamental parameters

1. Introduction

Observationally based estimates of the three-dimensional shapes of galaxies serve as a diagnostic of the physics of galaxy formation and evolution. Galaxies can only be seen in projection against the sky; thus, astronomers can only attempt to deduce their three-dimensional properties from their two-dimensional, projected properties. Obviously, information about intrinsic shapes is lost in projection; for instance, using only the two-dimensional surface photometry of a given galaxy, it is impossible to determine its intrinsic three-dimensional shape.

Elliptical galaxies have isophotes that are well approximated as ellipses (hence the name “elliptical”). The shape of an ellipse is specified by its axis ratio q , with $0 \leq q \leq 1$. The three-dimensional isophotal surfaces of elliptical galaxies are generally modeled as ellipsoids. A stellar system whose isophotal surfaces are similar, concentric ellipsoids, without axis twisting, will have projected isophotes which are similar, concentric ellipses, without axis twisting (Contopoulos 1956; Stark 1977). The apparent axis ratio q of the projected ellipses depends on the viewing angle and on the intrinsic axis ratios β and γ of the ellipsoid. Here, β is the ratio of the intermediate to long axis, and γ is the ratio of the short to long axis; thus, $0 \leq \gamma \leq \beta \leq 1$.

Beginning with Hubble (1926), many attempts have been made to deduce the distribution of intrinsic shapes of elliptical galaxies, given their distribution of apparent shapes. The early assumption, in the absence of evidence to the contrary, was that elliptical galaxies were oblate spheroids, flattened by rotation (Sandage, Freeman, & Stokes 1970). If elliptical galaxies were all oblate spheroids ($\beta = 1$), or all prolate spheroids ($\beta = \gamma$), and if their orientations were random, then it would be possible to deconvolve their distribution of apparent axis ratios $f(q)$, to find their distribution of intrinsic axis ratios $N(\gamma)$. However, the pioneering work of Bertola & Capaccioli (1975) and Illingworth (1977) led astronomers to abandon the assumption that elliptical galaxies are necessarily oblate. The shapes of ellipticals have been reanalyzed with the assumption that they are intrinsically prolate or triaxial, rather than oblate (Binney 1978; Benacchio & Galletta 1980; Bingelli 1980; Binney & de Vaucouleurs 1981; Ryden 1996).

Statements about the intrinsic shapes of galaxies must be statistical in nature, since astronomers do not exactly know the distribution $f(q)$ of axis ratios for a given class of galaxy. In this paper, we will be examining the apparent axis ratios for galaxies in the Sloan Digital Sky Survey (hereafter SDSS; York *et al.* 2000). The set of axis ratios we analyze constitute a finite sample drawn from a parent population $f(q)$. In this paper, we take into account the finite size of the sample in rejecting or accepting, at a known confidence level, two null hypotheses: that the galaxies are randomly oriented oblate spheroids, or that they are randomly oriented prolate spheroids. To accomplish this, we make a kernel estimate, $\hat{f}(q)$, of the distribution of axis ratios and mathematically invert $\hat{f}(q)$ to find $\hat{N}_o(\gamma)$ and $\hat{N}_p(\gamma)$, the estimated distribution of intrinsic axis ratios for a population of oblate spheroids and a population of prolate spheroids, respectively.

The rest of the paper is organized as follows. In section 2, we describe the Sloan Digital Sky Survey, and the methods by which the apparent axis ratios of the galaxies are estimated. In section 3, we present a brief review of the nonparametric kernel estimators used in this paper. In sections 4 and 5, we find the kernel estimate $\hat{f}(q)$ for galaxies with de Vaucouleurs

luminosity profiles and for galaxies with exponential profiles, and find the implications for their intrinsic shapes. In section 6, we discuss our results.

2. Data

The Sloan Digital Sky Survey is a digital photometric and spectroscopic survey which will, when completed, cover one quarter of the celestial sphere in the North Galactic hemisphere, and produce a smaller ($\sim 225 \square^\circ$) but much deeper survey in the South Galactic hemisphere. The photometric mosaic camera ((Gunn, *et al.* 1998) ; see also Project Book §4¹, “ The Photometric Camera”) images the sky by scanning along great circles at the sidereal rate. The imaging data are produced simultaneously in five photometric bands (u' , g' , r' , i' , and z' ; Fukugita *et al.* (1996)) with effective wavelengths of 3543, 4770, 6231, 7625, and 9134 Å².

In June 2001, the SDSS presented Early Data Release (EDR) to the general astronomical community, consisting 462 square degrees of imaging data in five bands. The data are acquired in three regions; along the celestial equator in the Southern galactic sky; along the celestial equator in the northern galactic sky; and in a region overlapping the Space Infrared Telescope Facility First Look Survey. Galaxies in the EDR were analyzed with the SDSS photometric pipeline *Photo* (Lupton *et al.* 2001). This code fits two models to the two-dimensional image of each galaxy. One model has a de Vaucouleurs profile:

$$I(r) = I_0 \exp(-7.67[(r/r_e)^{1/4}]) \quad (1)$$

which is truncated beyond $7r_e$ to go smoothly to zero at $8r_e$, and with some softening within $r_e/50$. The second model has an exponential profile:

$$I(r) = I_0 \exp(-1.68r/r_e) \quad (2)$$

which is truncated beyond $3r_e$ to go smoothly to zero at $4r_e$. Each model is assumed to have concentric isophotes with constant position angle ϕ and axis ratio q . Before the model is fit to the data, the model is convolved with a double-Gaussian fit to the point spread function (PSF). Assessing each model with a χ^2 fit gives r_e , q , and ϕ for the best-fitting model, as

¹<http://www.astro.princeton.edu/PBOOK/welcome.htm>

²We refer to the measured magnitudes in this paper as u^* , g^* , r^* , i^* , and z^* because the absolute calibration of the SDSS photometric system is still uncertain at the $\sim 0.03^m$ level. The SDSS filters themselves are referred to as u' , g' , r' , i' , and z' . All magnitudes are given on the AB_ν system (Oke & Gunn 1983). For additional discussion regarding the SDSS photometric system see Fukugita *et al.* (1996) and Fan (1999).

well as $P(\text{deV})$ and $P(\text{exp})$, the likelihood associated with the best-fitting de Vaucouleurs and exponential model, respectively.

We use the model fits in the r^* band to divide the galaxies into two classes: the “de Vaucouleurs” galaxies are those with $P(\text{deV}) > P(\text{exp})$ and the “exponential” galaxies are those with $P(\text{exp}) > P(\text{deV})$. In our data analysis we chose the likelihood $P > 10^{-5}$ for well behaved distribution of galaxies and the spectroscopic redshift $z < 0.2$, to reduce the effects of gravitational lensing of foreground objects. In addition, we require that a fit using one of the galaxy models is better than a pure PSF fit. The spectroscopic sample of the EDR contains 13092 de Vaucouleurs galaxies, and 6081 exponential galaxies, based on these criteria. Although the classification in the SDSS is based purely on the surface brightness profile, it is generally true that galaxies classified as “elliptical” in the standard morphological schemes are better fitted by de Vaucouleurs profiles than by exponential profiles (Kormendy & Djorgovski 1989), while galaxies morphologically classified as “spiral” are better fitted by exponential profiles.

The SDSS photometric analysis also provides an independent measure of the axis ratio; one based on the second moments of the surface brightness distribution. The Stokes parameters Q and U are given in terms of the flux-weighted second moments as

$$Q \equiv \langle x^2/r^2 \rangle - \langle y^2/r^2 \rangle \quad (3)$$

$$U \equiv \langle xy/r^2 \rangle \quad (4)$$

If the isophotes of the galaxy are indeed concentric ellipses of constant position angle and axis ratio, then the axis ratio q_{Stokes} is related to the values of Q and U by the relation

$$q_{\text{Stokes}} = \frac{\sqrt{Q^2 + U^2} - 1}{\sqrt{Q^2 + U^2} + 1}. \quad (5)$$

Unlike the axis ratios q_{model} found by fitting models, the values of q_{Stokes} do not attempt to correct for the effects of seeing.

For the galaxies in the SDSS EDR, the value of q_{Stokes} is generally larger than q_{model} as shown in Figure 1. To investigate the origin of this difference, we used the elliptical isophote fitting routine in Imaging and Reduction Analysis Facility (IRAF) to plot q versus r/r_e for a subset of galaxies in the sample. Figure 2 shows the result for just four of the de Vaucouleurs galaxies examined. The horizontal dashed lines indicate q_{Stokes} plus and minus the estimated error σ in q_{Stokes} ; the horizontal dotted lines indicate q_{model} plus and minus the estimated error σ in q_{model} . For these four galaxies, as for most galaxies in the SDSS, q_{Stokes} is greater than q_{model} . As is also typical, $q(r)$ found by fitting individual isophotes decreases as a function of radius; most elliptical galaxies are rounder in their central regions

than in their outer regions (Ryden, Forbes, & Terlevich 2001). The values of q_{Stokes} , based on the luminosity-weighted second moments, are primarily indicating the axis ratio of the central regions of each galaxy, where the surface brightness is highest. The values of q_{model} , by contrast, are more strongly influence by the axis ratio in the outer regions. Since, in this paper, we are not primarily interested in the central regions of the galaxies, we will adopt q_{model} as our primary measure of the axis ratio.

The distribution of galaxies in the SDSS EDR is strongly bimodal in the $g^* - r^*$ versus $u^* - g^*$ color-color diagram (Strateva *et al.* 2001). The optimal color separation between the two peaks is at $u^* - r^* = 2.22$. The detection of a local minimum indicates that the two peaks correspond roughly to early-type (E, S0) and late-type (Sa, Sb, Sc, Irr) galaxies. The late-type galaxies are the bluer group, reflecting their more recent star formation activity. The color criterion of Strateva *et al.* (2001) provides another means of dividing our data set. In addition to distinguishing between de Vaucouleurs and exponential galaxies, we can also distinguish between red ($u^* - r^* > 2.22$) and blue ($u^* - r^* \leq 2.22$) galaxies. Unsurprisingly, the de Vaucouleurs galaxies are predominantly red and the exponential galaxies are predominantly blue. Of the 13092 de Vaucouleurs galaxies, 10898 are red, but only 2194 are blue. Of the 6081 exponential galaxies, 4697 are blue, while only 1384 are red.

3. Method

We use a standard nonparametric kernel technique to estimate the distribution of intrinsic axis ratios. General reviews of kernel estimators are given by Silverman (1986) and Scott (1992); applications to astronomical data are given by Vio *et al.* (1994), Tremblay & Merritt (1995), and Ryden (1996). Here we give a brief overview, adopting the notation of Ryden (1996). Given a sample of axis ratios for N galaxies, q_1, q_2, \dots, q_N , the kernel estimate of the frequency distribution $f(q)$ is

$$\hat{f}(q) = \frac{1}{Nh} \sum_{i=1}^N K\left(\frac{q - q_i}{h}\right), \quad (6)$$

where $K(x)$ is the kernel function, normalized so that

$$\int_{-\infty}^{+\infty} K(x) dx = 1, \quad (7)$$

and h is the kernel width, which determines the balance between smoothing and noise in the estimated distribution. One way of choosing h is to use the value which minimizes the expected value of the integrated mean square error between the true f and the estimated \hat{f}

(Tremblay & Merritt 1995). We follow Silverman (1986) in using the formula

$$h = 0.9AN^{-0.2}, \quad (8)$$

with $A = \min(\sigma, Q_4/1.34)$, where σ is the standard deviation of the data and Q_4 is the interquartile range. This formula for h minimizes the expected value of the mean square error for samples which are not strongly skewed (Silverman 1986; Vio et al. 1994). We choose a Gaussian kernel, to ensure that \hat{f} is smooth and differentiable.

To obtain physically reasonable results, with $\hat{f} = 0$ for $q < 0$ and $q > 1$, we apply reflective boundary conditions (Silverman 1986; Ryden 1996). In practice, this means replacing the simple Gaussian kernel with the kernel

$$K_{\text{ref}} = K\left(\frac{q - q_i}{h}\right) + K\left(\frac{q + q_i}{h}\right) + K\left(\frac{2 - q - q_i}{h}\right). \quad (9)$$

Use of this kernel assures the correct normalization, $\int_0^1 \hat{f}(q) dq = 1$.

If we suppose that the N galaxies in our sample are randomly oriented oblate spheroids, then the estimated frequency of intrinsic axis ratios, $\hat{N}_o(\gamma)$ can be found by the mathematical inversion

$$\hat{N}_o(\gamma) = \frac{2\gamma\sqrt{1-\gamma^2}}{\pi} \int_0^\gamma \frac{d}{dq} \left(q^{-1} \hat{f} \right) \frac{dq}{\sqrt{\gamma^2 - q^2}}. \quad (10)$$

Similarly, if the galaxies are assumed to be randomly oriented prolate spheroids, the estimated frequency of intrinsic axis ratios, $\hat{N}_p(\gamma)$ is given by

$$\hat{N}_p(\gamma) = \frac{2\sqrt{1-\gamma^2}}{\gamma\pi} \int_0^\gamma \frac{d}{dq} \left(q^2 \hat{f} \right) \frac{dq}{\sqrt{\gamma^2 - q^2}}. \quad (11)$$

If the oblate hypothesis is incorrect, then the inversion of equation (10) may result in \hat{N}_o which is negative for some values of γ . Similarly, if the prolate hypothesis is incorrect, \hat{N}_p , from equation (11), may be negative.

To exclude the oblate or prolate hypothesis at some statistical confidence level, we must take into account the errors in \hat{f} both from the finite sample size and from the errors in measuring q for individual galaxies. The error due to finite sampling can be estimated by bootstrap resampling of the original data set. Randomly taking N data points, with replacement, from the original data set, a new estimator \hat{f} is created from the bootstrapped data, and is then inverted to find new estimates of \hat{N}_o and \hat{N}_p . After creating a large number of bootstrap estimates for \hat{f} , \hat{N}_o , and \hat{N}_p , error intervals can be placed on the original kernel estimates. In this paper, we did 300 bootstrap resamplings of each data set. An additional

source of error in \hat{f} , \hat{N}_o , and \hat{N}_p is the error that is inevitably present in the measured values of the apparent axis ratio. The SDSS EDR galaxies have an error σ_i associated with the axis ratio q_i of each galaxy. To model the effect of errors, we replace the kernel width h given by equation (8) with a broader width

$$h'_i = \sqrt{h^2 + \sigma_i^2}. \quad (12)$$

4. Galaxies with de Vaucouleurs Profiles

We can now apply the mathematical apparatus described in the previous section to our four subsamples of galaxies: red de Vaucouleurs galaxies, blue de Vaucouleurs galaxies, red exponential galaxies, and blue exponential galaxies. Unfortunately, given the desirability of large N in determining $f(q)$, not all the galaxies in the SDSS EDR are sufficiently well-resolved for their axis ratios to be reliably determined. A plot of q_{model} versus r_e , measured in units of the PSF width (PSFW), as shown in Figure 3, reveals that the galaxies with $q_{\text{model}} = 1$ are mainly galaxies whose effective radius is not much larger than the PSF width (typically, $r_e \lesssim 2$ PSFW). For instance, Figure 4 shows the estimated distribution $\hat{f}(q_{\text{model}})$ for all the red de Vaucouleurs galaxies ($N = 10,898$). In addition to the main peak at $q_{\text{model}} \approx 0.80$, there is a secondary peak at $q_{\text{model}} = 1$. To eliminate these spuriously round, poorly resolved galaxies, we retain in our samples only those galaxies with $r_e > 2$ PSFW. After this purge of too-small galaxies, there are $N = 5659$ galaxies in the red de Vaucouleurs subsample, $N = 1784$ galaxies in the blue de Vaucouleurs subsample, $N = 815$ galaxies in the red exponential subsample, and $N = 2263$ galaxies in the blue exponential subsample.

The estimated distribution $\hat{f}(q_{\text{model}})$ for the edited subsample of red de Vaucouleurs galaxies (excluding galaxies with $r_e < 2$ PSFW) is shown as the solid line in the upper panel of Figure 5. Note that the secondary peak at $q_{\text{model}} = 1$ has disappeared. The dashed lines to either side of the solid line are the 80% confidence intervals, estimated by bootstrap resampling, while the dotted lines are the 98% confidence interval. The estimated distribution $\hat{N}_o(\gamma)$ of intrinsic axis ratios, given the oblate hypothesis, is shown in the middle panel of Figure 5. The 98% confidence interval drops below zero for $\gamma > 0.91$; thus the oblate hypothesis for this subsample of galaxies can be rejected at the 99% (one-sided) confidence interval. To produce as few nearly circular galaxies as are seen, there would have to be a negative number of nearly spherical oblate galaxies. The estimated distribution $\hat{N}_p(\gamma)$, given the prolate hypothesis, is shown in the bottom panel of Figure 5. The best estimate for \hat{N}_p , shown as the solid line, is positive everywhere. Thus, the surface photometry of the red de Vaucouleurs galaxies is consistent with their being a population of randomly oriented prolate

spheroids. If they are all prolate, their average intrinsic axis ratio is

$$\langle \gamma \rangle_p = \int_0^1 \gamma \hat{N}_p(\gamma) d\gamma = 0.608 . \quad (13)$$

Although the shape distribution for red de Vaucouleurs galaxies is consistent with the prolate hypothesis, it doesn't require prolateness. The galaxies could also be triaxial and produce the same distribution of apparent shapes.

Plots of \hat{f} , \hat{N}_o , and \hat{N}_p are given in Figure 6 for the 1784 blue de Vaucouleurs galaxies. Just as for the red de Vaucouleurs galaxies, the oblate hypothesis can be rejected at the 99% confidence level, due to the scarcity of nearly circular galaxies in projection. The prolate hypothesis, though, cannot be rejected at the 90% confidence level for this sample; see the bottom panel of Figure 6. If the blue de Vaucouleurs galaxies are prolate, then \hat{N}_p yields an average intrinsic axis ratio $\langle \gamma \rangle_p = 0.592$, only slightly smaller than that for red de Vaucouleurs galaxies. As measured by Kolmogorov-Smirnov (K-S) test, however, the distribution of q for blue de Vaucouleurs galaxies is significantly different from that for red de Vaucouleurs. The K-S probability from comparing the two samples is $P_{KS} = 3 \times 10^{-3}$; i.e., the two samples are different at the 99.7% confidence level.

5. Galaxies with Exponential Profiles

Unlike galaxies with de Vaucouleurs profiles, which are generally smooth ellipticals, galaxies with exponential profiles are generally spiral galaxies, containing nonaxisymmetric structures such as spiral arms and bars. Given such a large amount of substructure present in spiral galaxies, attempting to characterize their shape by a single axis ratio q is a gross oversimplification. Nevertheless, as long as it is not over-analyzed, the distribution $\hat{f}(q)$ contains useful information about the overall shape of exponential galaxies.

For instance, Figure 7 shows the estimated value of $\hat{f}(q_{\text{model}})$ for the 815 red exponential galaxies. The peak in \hat{f} is at $q_{\text{model}} \approx 0.27$, and relatively few red exponential galaxies have $q_{\text{model}} > 0.6$. The large apparent flattening of the galaxies in the red exponential subsample is a sign that they are not a population of randomly oriented disks. Instead, the sample preferentially contains edge-on, or nearly edge-on disks. The red color of galaxies in this subsample is not the intrinsic color of the stars, but rather is the result of internal reddening by dust in the galaxy's disk. For a typical edge-on spiral galaxy like NGC 4594, the maximum reddening $E(B-V)$ is 0.4 (Knapen *et al.* 1991). Then the corresponding reddening in the $u-r$ color will be ~ 1 , using the transformation $E(u-r) = [A_u/E(B-V) - A_r/E(B-V)]E(B-V)$ with $A_u/E(B-V) = 5.155$ and $A_r/E(B-V) = 2.751$ (Stoughton *et al.* 2001).

By contrast, Figure 8 shows the estimated value of $\hat{f}(q_{\text{model}})$ for the 2263 blue exponential galaxies. The apparent shapes of blue exponential galaxies are very different from the apparent shapes of red exponential galaxies; a K-S test comparing the two populations yields $P_{\text{KS}} = 5.10^{-95}$. The scarcity of exponential galaxies with $q \gtrsim 0.9$ is an indication that the exponential galaxies are not perfectly axisymmetric disks. Indeed, visual inspection of the SDSS images reveals that most of the exponential galaxies contain readily visible nonaxisymmetric structure, in the form of spiral arms, bars, or tidal distortions.

6. Discussion

The galaxies in the SDSS EDR with de Vaucouleurs profiles have a distribution of apparent shapes which is incompatible (at the 99% confidence level) with their being randomly oriented oblate spheroids. This is consistent with the result found by Lambas, Maddox, & Loveday (1992) for a sample of 2135 elliptical galaxies with shapes estimated from survey plates of the APM Bright Galaxy Survey. When the SDSS survey is complete, it will provide a sample of galaxies ~ 20 times larger than the SDSS EDR. This increase in sample size will enable us to determine more accurately the distribution of apparent axis ratios $f(q)$. The kernel width h will be decreased by a factor $\sim 20^{-0.2} \sim 0.55$. The error intervals, which are essentially determined by the $N^{1/2}$ fluctuations in bins of width h , will be reduced by a factor $\sim 20^{-0.4} \sim 0.30$. Although a simple increase in the sample size will not enable us to determine the true distribution of intrinsic shapes, it will enable us to make stronger statistical statements about our rejection or acceptance of the prolate or oblate hypothesis.

The blue de Vaucouleurs galaxies, with a mean axis ratio of $\langle q_{\text{model}} \rangle = 0.639$, are only slightly flatter in shape than the red de Vaucouleurs galaxies, with $\langle q_{\text{model}} \rangle = 0.652$. Thus, if the color of the blue de Vaucouleurs galaxies is the result, at least in part, of recent star formation, we can conclude that the overall shape of the galaxies is not strongly affected by star formation. Although elliptical galaxies with old stellar populations tend to be rounder than those with young stellar populations (Ryden, Forbes, & Terlevich 2001), this difference is only large at small radii ($r \lesssim r_e/8$), while the values of q_{model} used in this paper emphasize the axis ratio at much larger radii ($r \gtrsim r_e$).

The galaxies with exponential profiles have, by contrast, shapes which are strongly dependent on color, with the red exponential galaxies consisting predominantly of dust-reddened edge-on (or nearly edge-on) disks. A significant number of galaxies in the SDSS EDR appear to be edge-on late-type galaxies, with exponential profiles, rather than early-type galaxies, with de Vaucouleurs profiles. The number of red exponential galaxies ($N = 815$) is 14.4% of the number of red de Vaucouleurs galaxies ($N = 5,659$). Thus, if we

attempted to select out elliptical galaxies purely on the basis of color, we would have been faced with a significant contamination by reddened disks. Spectroscopy or accurate surface photometry are required to distinguish between elliptical galaxies and disk galaxies. This analysis agrees very well with the result of Schade *et al.* (1999) and carries substantially more statistical weight.

In summary, galaxies with de Vaucouleurs profile have an axis ratio distribution consistent, at a high confidence level, with their being randomly oriented prolate spheroids (though it is also consistent with their being triaxial systems). Galaxies with exponential profiles have an axis ratio distribution which is dependent on color, suggesting that red exponential galaxies are nearly edge-on systems reddened by dust. Since a fair number of red galaxies in the SDSS EDR are nearly edge-on exponential disks, it is dangerous to select elliptical galaxies purely on the basis of color.

We wish to thank Ani Thakar for his assistance in downloading the data, and Brian Yanny, Jordi Miralda-Escudé, Richard Pogge and David Weinberg for their valuable suggestions. The Sloan Digital Sky Survey (SDSS) is a joint project of The University of Chicago, the Institute of Advanced Study, the Japan Participation Group, the Max-Planck-Institute for Astronomy (MPIA), the Max-Planck-Institute for Astrophysics (MPA), New Mexico State University, Princeton Observatory, the United States Naval Observatory, and the University of Washington. Apache Point Observatory, site of the SDSS telescopes, is operated by the Astrophysical Research Consortium (ARC). Funding for the project has been provided by the Alfred P. Sloan Foundation, the SDSS member institutions, the National Aeronautics and Space Administration, the National Science Foundation, the U.S. Department of Energy, the Japanese Monbukagakusho, and the Max Planck Society. The SDSS website is <http://www.sdss.org/>.

REFERENCES

- Benacchio, L., & Galletta, G. 1980, MNRAS, 193, 885
- Bertola, F., & Capaccioli, M. 1975, ApJ, 200, 439
- Binggelli, B. 1980, A&A, 82, 289
- Binney, J. 1978, MNRAS, 183, 501
- Binney, J., & de Vaucouleurs, G. 1981, MNRAS, 194, 679

- Contopoulos, G. 1956, *Z. Astrophys.*, 39, 126
- Fan, X. 1999, *AJ*, 117, 2528
- Fukugita, M., Ichikawa, T., Gunn, J. E., Doi, M., Shimasaku, K., & Schneider, D. P. 1996, *AJ*, 111, 1748
- Gunn, J. E., et al. 1998, *AJ*, 116, 3040
- Hubble, E. P. 1926, *ApJ*, 64, 321
- Illingworth, G. 1977, *ApJ*, 218, 43
- Knapen, J.H., Hes, R., Beckman, J.E. & Peletier, R.F. 1994, *A&A*, 241, 42
- Kormendy, J. & Djorgovski, S. 1989, *ARA&A*, 27, 235
- Lambas, D. G., Maddox, S. J., & Loveday, J. 1992, *MNRAS*, 258, 404
- Lupton, R. H., et al. 2001, in preparation
- Oke, J. B., & Gunn, J.E. 1983, *ApJ*, 266, 713
- Ryden, B. S. 1996, *ApJ*, 461, 146
- Ryden, B. S., Forbes, D. A., & Terlevich, A. I. 2001, *MNRAS*, 326, 1141
- Sandage, A., Freeman, K. C., & Stokes, N. R. 1970, *ApJ*, 160, 831
- Schade, D., et al. 1999, *ApJ*, 525, 31
- Scott, D. W. 1992, *Multivariate Density Estimation* (New York: Wiley)
- Silverman, B. W. 1986, *Density Estimation for Statistics and Data Analysis* (New York: Chapman & Hall)
- Stark, A. A. 1977, *ApJ*, 213, 368
- Strateva, I., et al. 2001, *AJ*, in press (astro-ph/0107201)
- Stoughton, C., et al. 2001, *AJ*, to be submitted
- Tremblay, B., & Merritt, D. 1995, *AJ*, 110, 1039
- Vio, R., Fasano, G., Lazzarin, M., & Lessi, O. 1994, *A&A*, 289, 640
- York, D. G., et al. 2000, *AJ*, 120, 1579

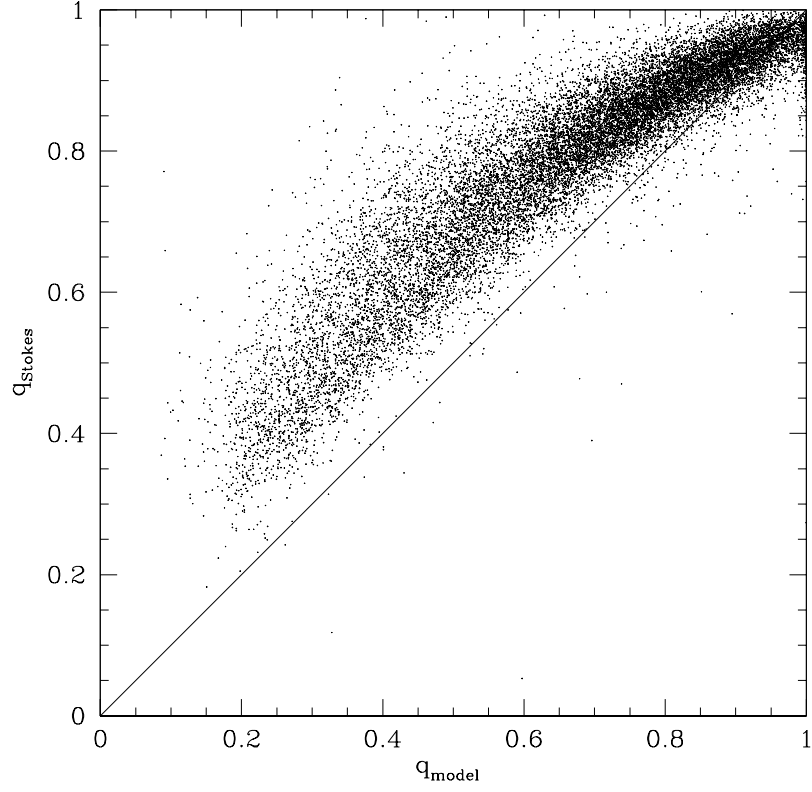


Fig. 1.— Axis ratio q_{Stokes} vs. axis ratio q_{model} for the galaxies studied.

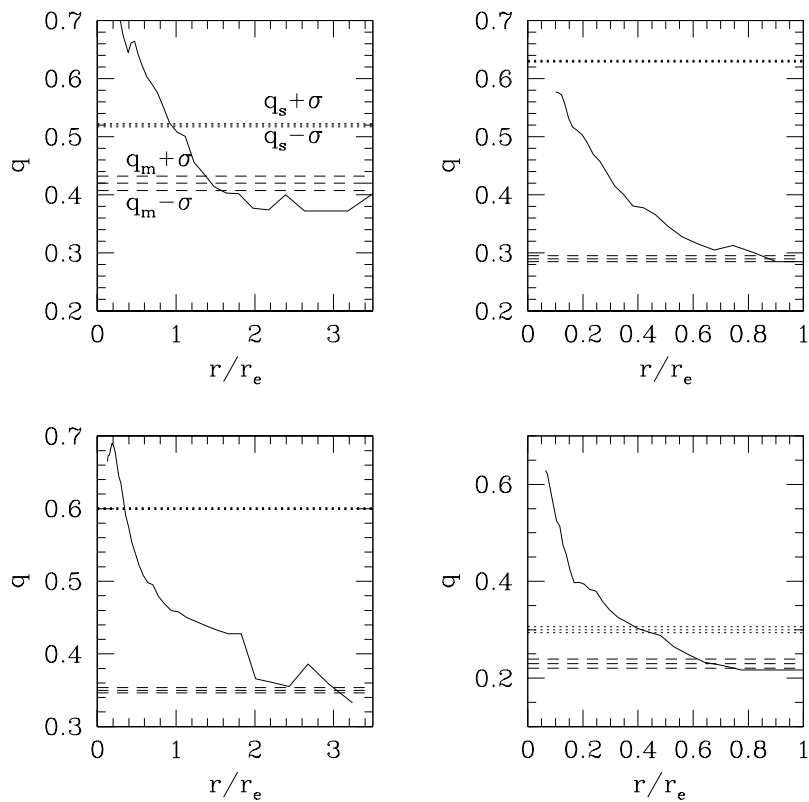


Fig. 2.— Axis ratio q as a function of r/r_e , for a sample of four de Vaucouleurs galaxies (two larger and two medium in size) in the SDSS. The solid line is the axis ratio found by the IRAF isophote fitting routine. The dotted lines represent q_{Stokes} plus and minus the associated error σ . The dashed lines represent q_{model} plus and minus the associated error σ .

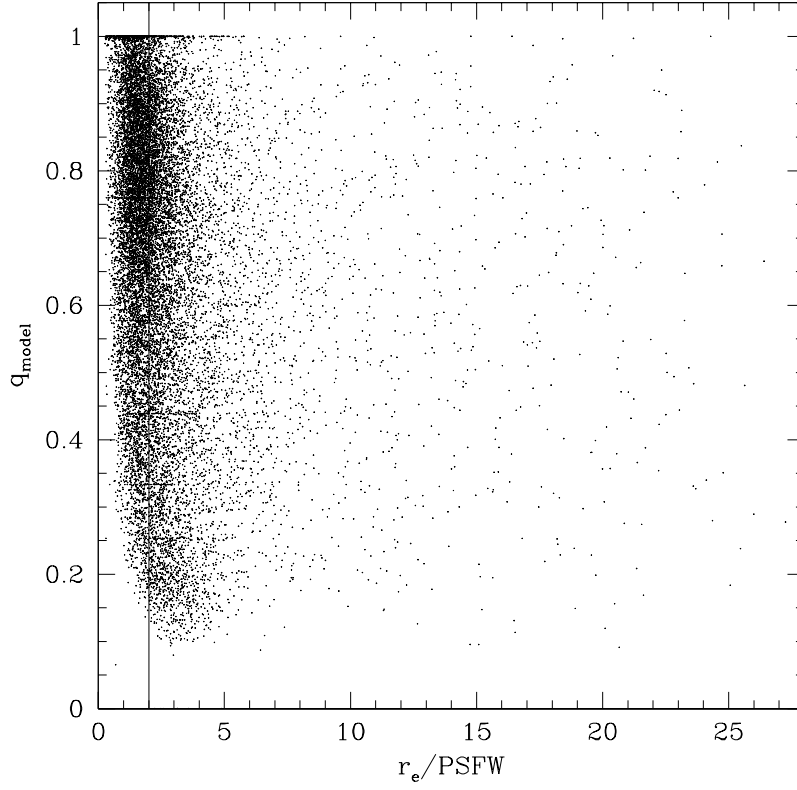


Fig. 3.— Axis ratio ratio q as a function of effective radius, measured in units of the PSFW, for galaxies with both de Vaucouleurs and exponential profiles. The solid line is drawn at $r_e/PSFW = 2$.

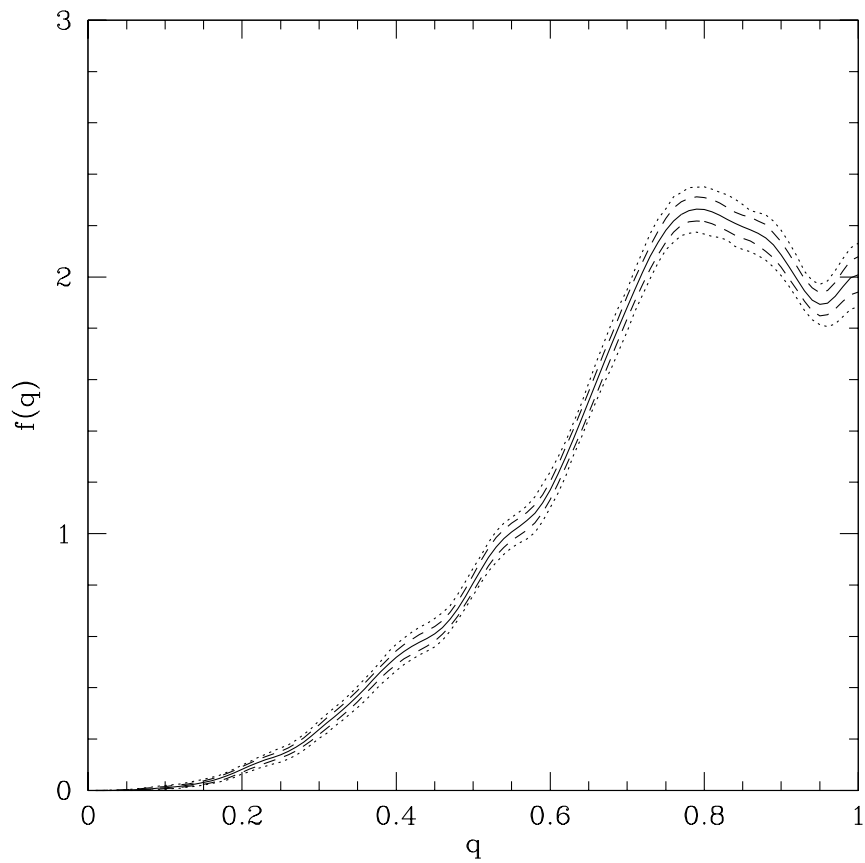


Fig. 4.— Nonparametric kernel estimate of the distribution of apparent axis ratios for the subsample of 10,898 red de Vaucouleurs galaxies. The kernel width is $h = 0.026$.

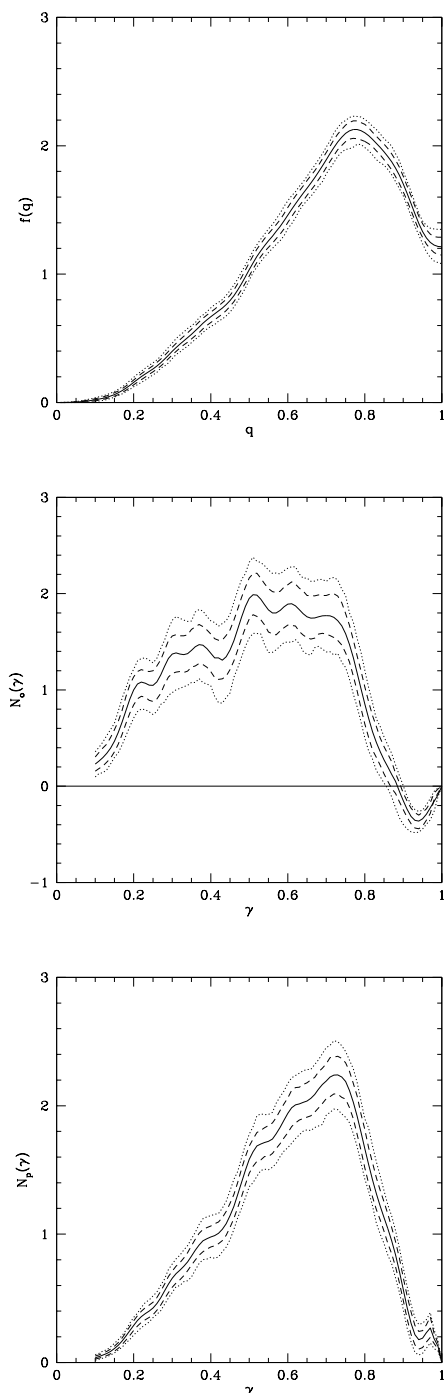


Fig. 5.— Top: The distribution of apparent axis ratios for a subsample of 5659 red de Vaucouleurs galaxies with $r_e > 2$ PSFW. Middle: The distribution of intrinsic axis ratios for the same subsample, assuming the galaxies are randomly oriented oblate objects. Bottom: The distribution of intrinsic axis ratios, assuming the galaxies are randomly oriented prolate objects. The kernel width is $h = 0.03$. The solid line in each panel is the best fit, the dashed lines give the 80% error interval, and the dotted lines give the 98% error interval.

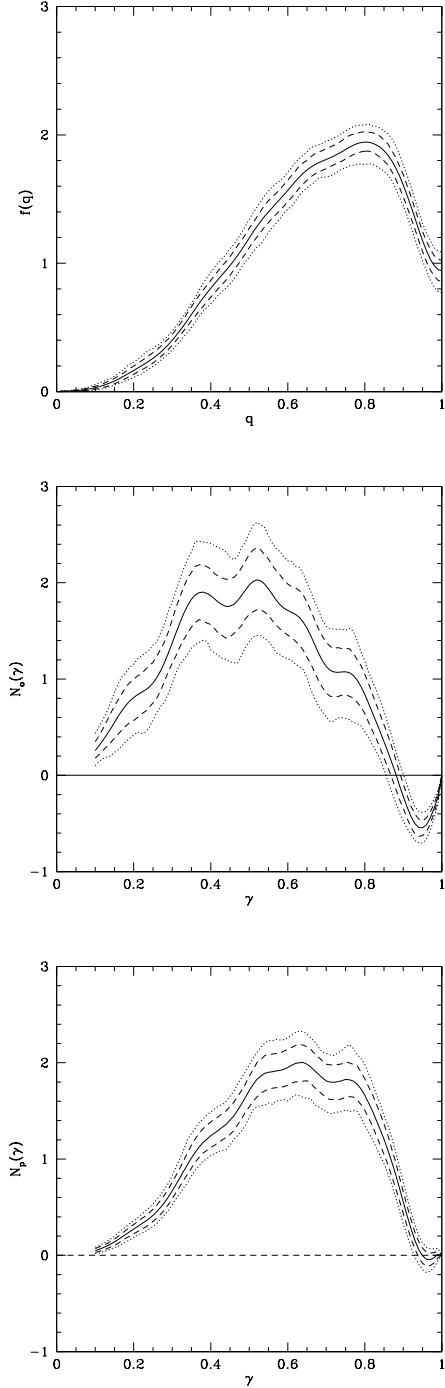


Fig. 6.— As in Figure 5, but for a subsample of 1784 blue galaxies well fit by a de Vaucouleurs profile. The kernel width is $h = 0.042$.

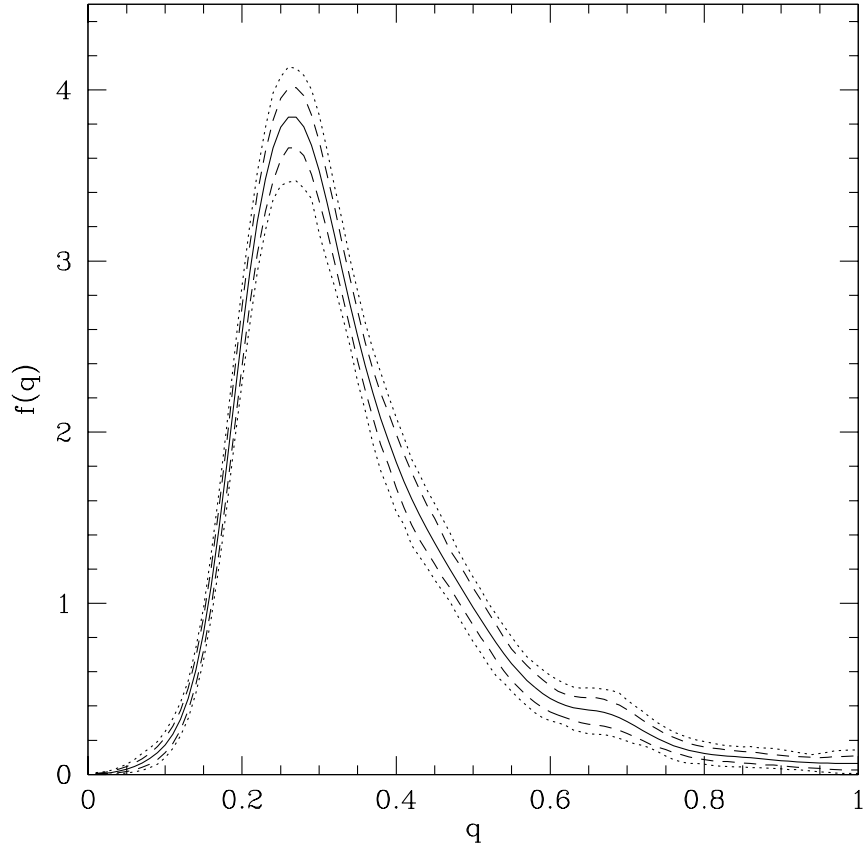


Fig. 7.— The distribution of apparent axis ratios for a subsample of 815 red galaxies well fit by an exponential profile (only galaxies with $r_s > 2PSFW$ are included). The kernel width is $h = 0.040$.

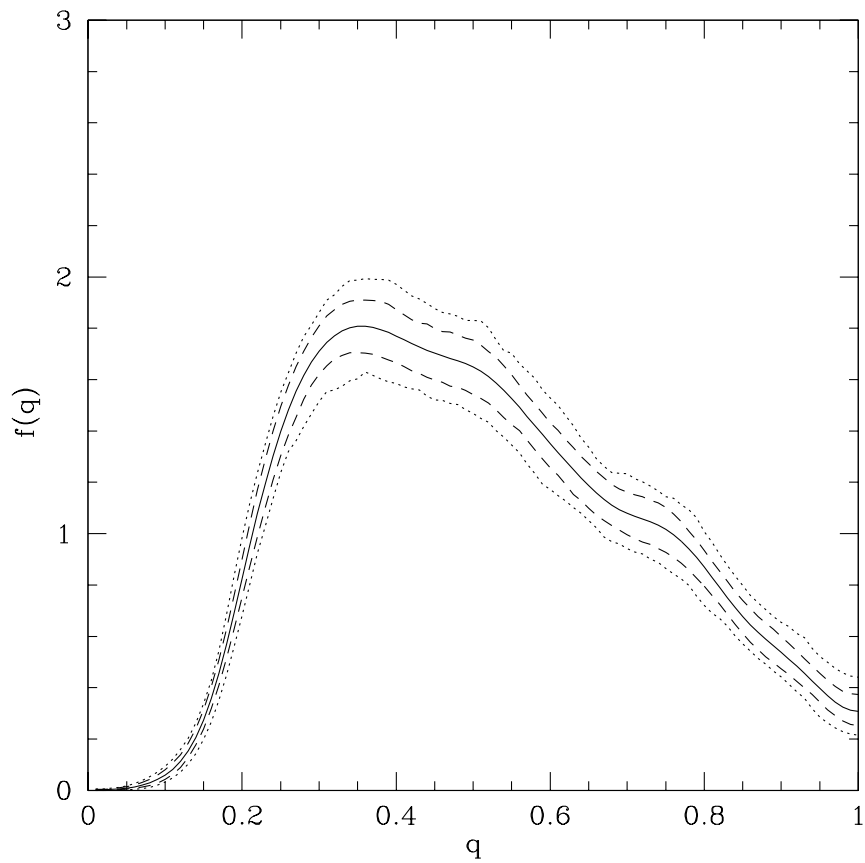


Fig. 8.— As in Figure 7, but for a subsample of 2263 blue galaxies well fit by an exponential profile. The kernel width is $h = 0.038$.